Paper No. 211

ISMS 2016

Estimating stope vein footwall stability using various constitutive modelling techniques

Andrew Pyon, Atsushi Sainoki, Hani S. Mitri

Department of Mining and Materials Engineering, McGill University, Montreal, Canada, H3A 0E8

ABSTRACT

Operating in weak narrow vein mines presents many issues in terms of ore productivity. Maintaining stable mining excavations and limiting unplanned overbreak are some of the main concerns in narrow vein mining. The use of numerical modelling has become a popular method because it is capable of examining stress patterns and identifying rockmass failure. This paper will focus on creating a 3-dimensional constitutive numerical model for narrow vein mines that incorporate weak rockmass properties. The selected Case Study Mine is an underground narrow vein mine joining a weak material known as talc-chlorite-schist. The construction of this model will be associated with the unplanned ore dilution determined by surveyed profiles from the mine site.

KEYWORDS: Numerical modelling; ore dilution; rock mechanics; underground mining; footwall stability; failure criterion

1. INTRODUCTION

The selected Case Study Mine, located 50 km west of Val d'Or, Quebec, Canada, was chosen for this study as it held a weak rockmass known as talc chlorite schist that presented important stability issues in the stopes. Over the course of its operations, the existence of schist material represented 70% of ore dilution from planned stopes and over 1 metre of wall displacements from drifts due to squeezing ground. Such difficulties are not to be overlooked and are worth investigating.

2. ORE DILUTION IN NARROW VEIN MINING

Ore dilution is defined as the unsolicited waste rock caused by overbreak of stopes. A poor control of dilution will induce the extraction of excess waste materials, which will present more handling of the rock as well as unnecessary additional costs. Rock overbreak comes from several causes such as the quality of geology, ore continuity, planarity of the walls and dip of the orebody (McCarthy, 1993).

There are a number of approaches to establish overbreak benchmarks in stopes. The most common ones are related to the relaxation of stope surfaces. Relaxation typically occurs when tensile stresses are created through opening of existing joints or the creation of new cracks formed by induced stresses (Potvin, 1988). It is therefore projected that once the rockmass exhibits mining-induced tensile stresses, unplanned dilution occurs. This is stated as $\sigma_3 \leq 0$, i.e. when σ_3 is tensile. Other dilution criteria related to relaxation are: 1) $-\sigma_3 \leq \sigma_t$, i.e. when σ_3 is tensile and is lower than the tensile strength, and 2) when the rockmass yields (Zniber, et. al., 2009). However, dilution can take many other forms of failure such as spalling, bending, wedge failure, crushing, etc. A combination of these failure modes is also possible leading to complex dilution occurrences. During the process of applying various numerical constitutive models, failure conditions will be examined to get a better grasp of rock behaviour.

3. CASE STUDY MODEL

The Case Study Mine is located within the Cadillac-Larder Lake Fault Zone. This zone contains the Archean-age Piché Volcanic rock in which many of the gold-mineralized structures are inside the hinges of the folds. There are 2 central groups of rockmasses where mining will be detained. One is the Piché group containing mafic to ultra-mafic talk-chlorite schist combined with intrusive volcanic rocks such as basalt. This group is known to be highly anisotropic in which the rockmass is extremely foliated.

The second group is called the Cadillac group comprised mostly of fine grained sedimentary Greywacke. The orebody is situated between these two rockmasses with widths varying between 3 to 8 metres and 85° dip.

*Pyon, A. – email: andrew.pyon@mail.mcgill.ca



Figure 1: Foliated schistose rockmass in footwall buckling towards the drift (Case Study Mine).

4. METHODOLOGY

4.1 NUMERICAL MODELLING SOFTWARE: FLAC3D

To perform an in depth dilution analysis in a 3-dimensional medium, FLAC3D (Fast Lagrangian Analysis of Continua) was selected. This software is a 3-D finite-difference program that uses well defined numerical formulations between geotechnical materials (Itasca, 2012). Geometric models are arranged by polyhedral elements in which failure laws are given based on elastic or plastic behaviours. The main advantage of using this tool is its ability to accurately represent the effect of plasticity in a 3-D medium. This is most suitable for ductile materials similar to the case of the Piché group at the Case Study Mine.

4.2 MODEL SETUP

Since the rockmass structures are fairly continuous at steep dips, it is best to construct the model into layers. 4 sections have been assigned to distinguish the main alterations within the heterogeneous nature of the rockmass. These are *Volcanic Zone*, *Orebody Zone*, *Weak Schist Zone* and *Sediment Zone*. Each of these layers consists of different rock compositions based on geological mapping of the Case Study Mine. The extents of these zones are defined when there are prominent changes in the arrangements of the rock. The model is designed as a brick and each boundary is widened to at least 5 times the size of one stope allowing calibration for far field stresses. Smaller meshes were applied in the area of interest and were gradually enlarged towards the boundaries. Meshes were adjusted until displacements and stresses converged to a stable state. The final model contains 1,234,800 elements.

The stope of interest for this study is at a depth of 1040 metres from ground level. A Cavity Monitoring System (CMS) was used to survey the overbreak approximately one week after blasting. Figure 2a shows a section view of the mined stope profile. As can be seen, significant footwall dilution and little hangingwall dilution took place. This is mainly because of the strong volcanic hangingwall basalt rock. Cablebolts were installed in the drift sidewalls. It is worth noting that other influences such as stope undercut, blasting and drilling were not accounted for in this model. The model contains sill drifts in between openings. Stopes are located midpoint of the *Orebody Zone* in which it dips at an angle of 85° south. Figure 2b shows the final isotropic view of the model along with its dimensions.

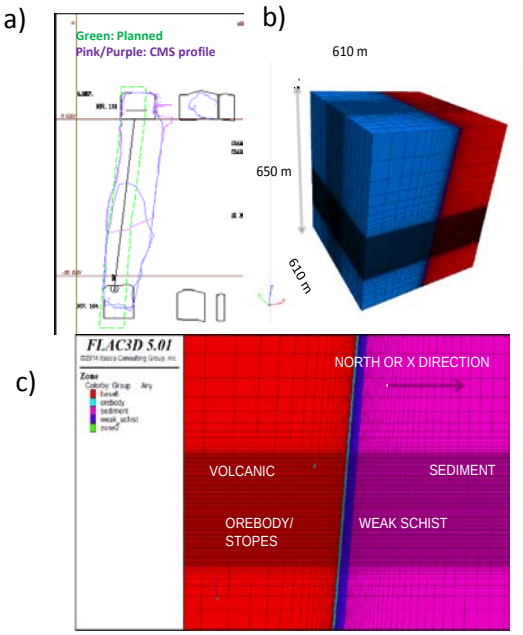


Figure 2: Case Study Mine Model a) Surveyed profile of the stope b) Perspective view c) Side view against the x-axis.

4.3 ROCKMASS CLASSIFICATION OF CASE STUDY MINE

Based on laboratory tests and field observations, rockmass parameters have been compiled into a database. Uniaxial compressive strength tests (UCS) were performed on intact core samples to acquire UCS values, the intact Young's Modulus of Elasticity (E_i), poisson's ratio (ν) and intact Hoek & Brown fit parameter (m_i). The Damage Factor (D) was also obtained from underground field observations.

Rock samples were classified as Sedimentary Wacke rocks, Intrusive Volcanic rocks and Schistose

rocks. Once compiled into a database, Hoek & Brown parameters are calculated to translate into equivalent rockmass values (Hoek & Brown, 2002). These were further converted into Mohr-Coulomb parameters with a best-fit linear relationship between major and minor principal stresses. Doing so, attaining equivalent equations for the angle of friction (ϕ'), cohesive strength (c') and tensile strength (σ_t') for each rockmass are made possible.

FLAC3D also requires using elastic constants such as Bulk Modulus (K) and Shear Modulus (G) to specify volumetric change and shear resistance of rocks. These are found by incorporating the Young's Modulus of Elasticity for the rockmass (E_{rm}) and Poisson's ratio (ν):

$$K = \frac{E_{rm}}{3(1-2\nu)} \quad (1)$$

$$G = \frac{E_{rm}}{2(1+\nu)} \quad (2)$$

The dilation angle (ψ), a function of volumetric change, is measured as $\psi = \frac{\phi'}{4}$.
The final rockmass properties are given in Table 1.

4.4 IN-SITU STRESSES

In order to reach a more realistic approach, stresses were applied on the boundaries of the numerical model. Doing so, an uneven distribution of internal stresses will travel through the different layers of rock. Stresses will be re-adjusted depending on the properties of each material before moving on to the next (R.P. Bewick, 2009). The applied stresses were adapted to stress tensor results that were previously measured (Arjang, 1996). The bottom boundary is fixed with rollers and vertical stress (σ_v) was applied on top with the following equation:

$$\sigma_V = \gamma H \quad (3)$$

Where γ is the average unit weight of the rockmass in MN/m3 and H is the depth of the mine. Additionally, stresses were applied on the x and y axes until the tensor values were achieved. The tensor is at a depth of 900 metres below surface with $\sigma_{maximum}$=51.8 MPa, $\sigma_{intermediate}$=35.8 MPa and $\sigma_{minimum}$=19.0MPa. This was assumed to be positioned at coordinates x=300, y=305 and z=350 in the *Sedimentary Zone* of the model. It was also ensured that this tensor was within 300 metres of model boundaries to account for far field stresses. The final stresses that were applied on the boundaries were determined to be σ_{xx}=50MPa, σ_{yy}=21 MPa and σ_{zz}=18 MPa.

5. NUMERICAL STRESS RESULTS

Before moving on, it was necessary to examine the stress fields before selecting a representative constitutive model. FLAC3D's *Ubiquitous Joint Model* was selected for the weak material since it accounts for plasticity and anisotropic behaviour of the rockmass. All other rock zones will be evaluated as isotropic elastic models due to its brittleness.

When excavating the first primary stope, lower stresses (-2 to 25 MPa) are observed in the *Weak Schist Zone* while high stresses (20 to 50MPa) are in the host rocks. Note that in FLAC3D, negative numbers refer to compressive stresses and positive numbers refer to tensile stresses. The major (σ_1) and intermediate (σ_2) principal stresses have relatively similar values in the schistose zone (0 to 25 MPa). As for the minor principal stresses (σ_3), few pockets of negative stresses are observed on the footwall face. This shows the presence of relaxation occurring in the abutment's surface.

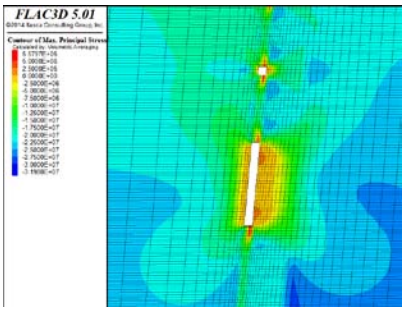


Figure 3: Post-mining section view of minimum principal stresses (σ_3).

The directions of these stresses were also perceived by looking at the σ_{xx}, σ_{yy} and σ_{zz} contours of the model. The stress contours in the y-axis (σ_{yy}) of the model displays the highest values which depicts the maximum principal stresses. The stresses in vertical direction (σ_{zz}) correlate with the intermediate principal stresses. The stress contours in the x-axis (σ_{xx}) shows the lowest, hence, minimum principal stresses.

Table 1: Selected rockmass parameters for numerical modelling study.

	HW Basalt	Orebody	FW Weak Schist	Sediment Wacke
Young's Modulus (E_{rm}) GPa	18.9	7.29	2.17	23.3
Bulk Modulus (K_{rm}) GPa	9.27	3.8	1.13	1.14
Shear Modulus (G_{rm}) GPa	8.15	3.09	0.92	10
Cohesion (c) MPa	4.9	2.7	2.2	4.3
Friction Angle (ϕ)°	44.2	31.5	27	42.7
Dilation (ψ)°	11	7.88	6.8	10.68
Tensile Strength (σ_t)	-0.3	-0.05	-0.05	-0.2
Poisson's Ratio (ν)	0.16	0.18	0.18	0.16

From these observations, the highest stresses occur in the y and z directions, both parallel to the footwall abutment. This suggests that a spalling or a slabbing type failure might arise.

6. DILUTION FAILURE MODES AT CASE STUDY MINE

6.1 RELAXATION (TENSILE) FAILURE

As previously mentioned, relaxation of rock occurs when the expansion of joints loosens the rock and falls off due to gravity pull. In this model, the failure criterion is expressed as $\sigma_3<0$. FLAC3D's *Elastic Transversally Isotropic* (*Anisotropic*) model was chosen for the *Weak Schist Zone*. A Young's modulus ratio of 1 to 7 was chosen in direction perpendicular to the planes of weakness. Figure 4 shows the areas of relaxation (in red) and the CMS profile of the first excavated primary stope (in white). A fine layer of tensile failure is observed in the footwall which is underestimating CMS results. This method is thus not recommended to analyze ore dilution in weak rock properties. Although tension is clearly shown in field observation, the rock's ductile behaviour renders the no-tension model ineffective.

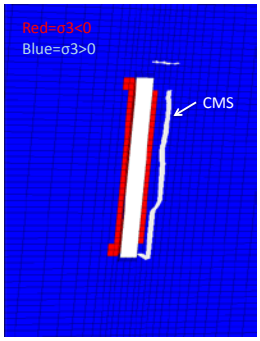


Figure 4: No-tension ($\sigma_3<0$) analysis in elastic transversally isotropic (anisotropic) model.

6.2 BIAXIAL FAILURE

Biaxial failure occurs when poly-axial loading near rock surface causes an accumulation of mining-induced planar stresses (Yun et. al., 2010). This in turn can cause a wide variety of failures such as spalling, slabbing, buckling and crushing. An *Elastic Transversally Isotropic (Anisotropic)* constitutive model was selected in order to account for high stresses and disregarding the effect of material's peak strength. σ_1 and σ_2 results show that the tensor values in the *Weak Schist Zone* range from 0 to 90 MPa. These values were then plotted in order to see if a failure pattern exist. Figure 5 illustrates a σ_1/σ_c versus σ_2/σ_c plot where σ_c represents the UCS of intact rock. Tensors were grouped by their σ_3 values and divided by σ_c for normalization purposes.

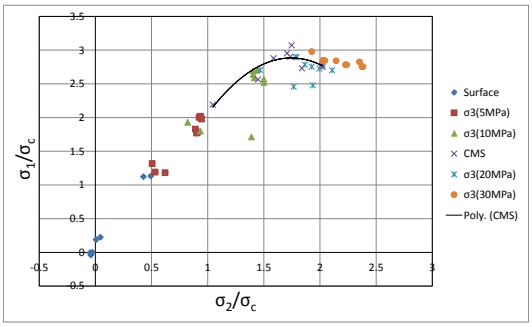


Figure 5: σ_1/σ_c vs σ_2/σ_c tensors along footwall width.

An increase in biaxial stresses was observed as it went deeper into the footwall. With an increase in σ_2, σ_1 rises until it reached equilibrium of 90 MPa. A best fit polynomial was then conducted for tensors along the CMS overbreak profile which showed that σ_3 ranges from 10 MPa to 30 MPa. Given that the ranges of biaxial stresses along the overbreak outline are $2.19 < \sigma_1/\sigma_c < 3.07$ and $1.04 < \sigma_2/\sigma_c < 2.02$, it can be made possible to evaluate dilution profiles in

foliated talc-chlorite-schist as a result of biaxial loading. However, further models are needed to validate these results.

6.3 SHEAR AND TENSILE YIELDING

Shear or tensile yielding was analyzed by conducting a *Ubiquitous Joint Model*. This constitutive model takes into consideration planes of weakness on a perfectly elasto-plastic Mohr-Coulomb model. Failure criteria are designated by its Mohr-Coulomb envelopes as well as the weak-plane of failure. Additional joint properties were employed which were dramatically reduced from the rockmass properties (0.5 MPa for joint cohesion and 12° for joint friction angle). This was done to reflect the utmost critical joint conditions. Figure 6 shows the yielding states on the model before excavation.

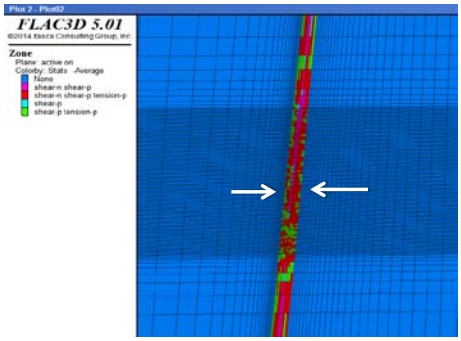


Figure 6: Yielded states of Case Study Mine model before excavation with directions of applied loads.

The weak material undergoes shear and tensile yielding in its entirety as indicated by the green, red, purple, cyan and pink colors (the "-n" in the legend signifies failure now and "-p" signifies failure in past iterations). This is primarily due to the effect of having weak material constrained within stronger materials. The arrangement of rocks will cause high loads on the weaker material, which results in yielding. Evaluating shear or tensile yield in response to dilution is therefore not desirable since yielding has occurred prior to excavations.

6.4 EFFECTIVE PLASTIC STRAIN FAILURE

The *Effective Strain* is defined as the amount of body rotation and distortion due to deviatoric principal strains. Uneven amounts of strains in the principal directions can cause the material to change its shape and volume. This behaviour can ultimately obstruct the rockmass and result in dilution. The *Equivalent Total Strain* (ε_ε) is calculated according to the following equation (Xia and Wang, 2001):

$$\varepsilon_\varepsilon = \sqrt{\frac{2}{9}\left[(\varepsilon_x - \varepsilon_y)^2 + (\varepsilon_y - \varepsilon_z)^2 + (\varepsilon_z - \varepsilon_x)^2\right] + \frac{1}{3}(\gamma_{xy}^2 + \gamma_{yz}^2 + \gamma_{zx}^2)} \quad (4)$$

Where:

ε_x, ε_y and ε_z = total principal strain in the x, y and z-axis, respectively.

γ_{xy}, γ_{yz} and γ_{zx} = total shear strain in xy plane, yz plane and zx plane respectively.

For this analysis, the *Ubiquitous Joint model* was selected to account for the plasticity of the rockmass and planes of failure. Given that the material behaves as a perfectly-elasto plastic model, it is essential to determine at what strain amount will be affected by dilution. Since failure occurs when there is permanent or irreversible strain in the material, it is required to measure the amount of strain from the point of yield stress to the point of dilution as shown in Figure 7, which is also known as the *Equivalent Plastic Strain* or E.P.S.

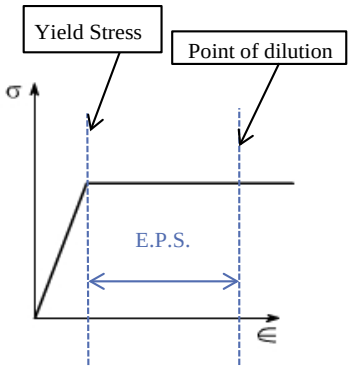


Figure 7: Illustration of perfectly elasto-plastic curve and applied E.P.S.

The *Effective Plastic Strain* generated amounted to 15% to achieve the CMS overbreak profile as shown in Figure 8.

Although the use of *Effective Plastic Strain* gives fair results in identifying ore dilution, more studies are needed for validation; especially since the geological and mining conditions fluctuate at varying depths.

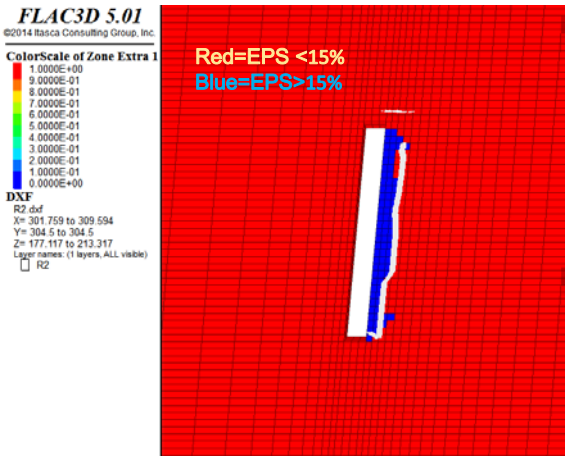


Figure 8: Comparison of CMS profile with 15% Effective Plastic Strain (midpoint).

7. CONCLUSIONS

The no-tension model proves to be ineffective due to the minimal tensile in the footwall. However, failure under biaxial loading condition is noticeable due to the stresses applied on the stope footwall face. This needs to be validated with other stope models for future studies. From the *Ubiquitous Joint Model*, the shear and tensile yields cannot be implemented since yielding states occur at pre-mining stages. This event is primarily caused from the application of high loads of the stronger rockmasses into the *Weak Schist Zone*. Finally, the *Effective Plastic Strain* has been examined. The actual (measured) overbreak of the stope corresponds to 15% *Effective Plastic Strain*. Although these results are encouraging, further studies are needed to validate this method.

8. ACKNOWLEDGEMENT

This research paper was made possible through the help and support from the members of the McGill Mine Design Lab team.

9. REFERENCES

Arjang, B., (1996). In situ ground stresses in the Abitibi Mining District. CIM Bulletin, 89, no. 996, p.65-71.

Bewick, R.P., Valley, B. and Runnalls, S. (2009). Global Approach to Managing Deep Mining Hazards, Proceedings of the 3rd CANUS Rock Mechanics Symposium, Toronto, May 2009, Paper 3994

Brewis, T. (1995). Narrow Vein Mining 1 – Steep Veins. Mining Magazine. Vol.173, No.3, pp.116-130

Henning, J. and H.S. Mitri (2007). Numerical modeling of ore dilution in blasthole stoping. International Journal of Rock Mechanics and Mining Sciences. Res. 44: 5, pp. 692-703

Hoek, E., C.T. Carranza-Torres and B. Corkum. (2002). Hoek-Brown failure criterion - 2002 edition. In Proceedings of the Fifth North American Rock Mechanics Symposium and 17th Tunneling Association of Canada Conference, Toronto, 7-10 July 2002, pp. 267-273

ITASCA (2012). FLAC3D - Fast Lagrangian Analysis of Continua. 5.0 ed. U.S.A.: Itasca Consulting Group Inc.

McCarthy, P. (1993). Economics of Narrow Vein Mining, Narrow Vein Mining Seminar, The Australasian Institute of Mining and Metallurgy, pp.89-97

Miller, F., Potvin, Y. and Jacob, D. (1992). Laser measurement for open stope dilution. CIM Bulletin 1992, pp.85:96-102

Potvin, Y., (1988). Empirical open stope design in Canada. PhD. Thesis, University of British Columbia, Vancouver

Xia, K. and Wang, J. (2001). Shear, Principal, and Equivalent Strains in Equal-Channel Angular Deformation, Metallurgical and Materials Transactions A, Volume 32A, pp.2639-2647

Yun et. al., (2010). Experimental Investigation into Biaxial Compressive Strength of Granite. International Journal of Rock Mechanics & Mining Sciences. 47. pp.334-341

Zniber, E. M., et. al. (2009). Effect of stope undercutting on its wall overbreak. Proceedings 43rd US Rock Mechanics Symposium, held in Asheville, NC June 28th – July 1, Paper No. ARMA 09-200